Journal of Inorganic and General Chemistry
ZAAC
Zeitschrift für anorganische und allgemeine Chemie
DOI: 10.1002/zaac.202000357
ARTICLE

Synthesis and Single Crystal Structure Characterization of Dinuclear and Polymeric Mixed-ligand Coordination Compounds of Zinc(II) and Cadmium(II) with the Bridging Ligand 1,2-Bis(pyridin-4-ylmethylene)hydrazine

Mahsa Armaghan,*[a] Ezzat Najafi,[b] Tim-Oliver Knedel,[a] Walter Frank,*[a] and Christoph Janiak*[a]

Dedicated to Professor Herbert W. Roesky on the Occasion of his 85th Birthday

Abstract. Three d^{10}-transition-metal coordination compounds $[Cd(tfpb)_2(4\text{-bpmh})]_n$ (**1**), $[Cd(9\text{-aca})(NO_3)(OHCH_3)(4\text{-bpmh})]_n$ (**2**) and $[Zn_2(dpp)_4(4\text{-bpmh})]$ (**3**) with the bridging ligand 4-bpmh were synthesized [4-bpmh = 1,2-bis(pyridin-4-ylmethylene)hydrazine, tfpb = 4,4,4-trifluoro-1-phenylbutane-1,3-dionate, 9-aca = anthracene-9-carboxylate, dpp = 1,3-diphenylpropane-1,3-dionate]. Compounds **1**–**3** were characterized by FT-IR spectroscopy, elemental analysis, and structurally authenticated by X-ray crystallography. Compounds **1**–**3** are constructed by an *O,O′*-donor ligand including chelating β-diketonates (tfpb, dpp) in **1** and **3** and a carboxylate ligand (9-aca) in **2** in combination with a linear neutral bidentate and bridging N-ligand (4-bpmh). The assembly and action of the bridging 4-bpmh ligand leads to one-dimensional coordination polymers in **1**, **2** and to a dinuclear coordination complex in **3**. The structures and the solid-state supramolecular interactions for studying the crystal packing fashions of **1**–**3** were analyzed. The supramolecular interactions including hydrogen bonding, C–H···π, π···π, and C–F···π in **1**, **2**, and **3** were founded.

Introduction

1,2-Bis(pyridin-4-ylmethylene)hydrazine (4-bpmh, Scheme 1)[1] is a neutral multidentate linker containing up to four N-coordination sites.[2,3] 4-bpmh usually plays a role as a long linear bridging ligand via both terminal pyridyl nitrogen atoms in dinuclear, polynuclear coordination compounds,[4,5] multi-dimensional coordination polymers (CPs),[6–19] and porous coordination polymers (PCPs).[20–37] Furthermore, it has been observed that 4-bpmh is able to undergo weak interactions to form supramolecular architectures.[38–40] 4-bpmh has recently been widely employed as a secondary ligand in the design and construction of mixed-ligand coordination compounds. From the literature survey and a Cambridge Structural Database (CSD) search, the function of 4-bpmh has been actively studied as a bidentate bridging ligand or a spacer in combination with other organic ligands in Zn^{2+} and Cd^{2+} (d^{10} metals) coordination compounds.

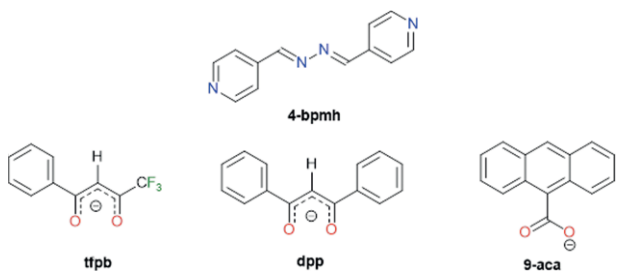

Scheme 1. Chemical structures of tfpb, dpp, 9-aca, and 4-bpmh.

The other organic ligands in combination with 4-bpmh in the library of mixed-ligand Zn^{2+} or Cd^{2+} coordination compounds were: S,S′-chelating (2-hydroxyethyl)(propyl)carbamodithioate (S_2CNR_2),[2] S,S′-diisopropyldithiophosphato,[4] 2-thiophenecarboxylate (2-tpc),[6] *para*-chlorobenzoate (*p*-clba), *para*-bromobenzoate (*p*-brba),[8] saccharinate ($C_7H_5NO_3S$, sac),[14] 2-amino-1,4-benzene dicarboxylate (2-NH_2-1,4-bdc),[21,35] 5-amino-1,3-benzene dicarboxylate (5-NH_2-1,3-bdc),[15] 1,3-benzenedicarboxylate (1,3-bdc), terephthalate (terep),[16,21,34] 5-nitroisophthalate (nip), 5-*tert*-butylisophthalate (tbip),[22] benzene-1,3,5-tri carboxylate (btc),[24] biphenyl-4,4′-dicarboxylate (bpdc),[27] isonicotinate ($C_6H_5NO_2$),[18] 9,9-dimethylfluorene-2,7-dicarboxylate (mfda), 9,9-diethylfluorene-2,7-dicarboxylate (efda),[19] 1,4-phenylene diacetate (1,4-

* Dr. M. Armaghan
E-Mail: armaghan@hhu.de
* Prof. Dr. W. Frank
E-Mail: wfrank@hhu.de
* Prof. Dr. C. Janiak
E-Mail: janiak@hhu.de
[a] Institute für Anorganische Chemie und Strukturchemie
Heinrich-Heine Universität
40204 Düsseldorf, Germany
[b] Department of Chemistry
Payame Noor University (PNU)
Tehran 19395–3697, Iran
Supporting information for this article is available on the WWW under **http://dx.doi.org/10.1002/zaac.202000357** or from the author.

pdaa), 1,3-adamantane diacetate (1,3-adaa),[20] 2,5-furandicarboxylate (fdc),[23] 4,4′-sulfonyldibenzoilate (sdb),[26] glutarate (glu), 3-methylglutarate (3m-glu), pimelate (pim), succinate (suc),[28] 4,4′-oxybis(benzoilate) (oba),[29,31,32,33] 4-(4-carboxyphenoxy)phthalate (cpop),[17] 4,4′-(hexaflouroisopropylene)bis(benzoilate) (hfipbba).[30]

Among these coordination compounds, several structure arrays have been observed and studied: the mononuclear structure in $[Cd(C_6H_{12}NOS_2)_2(4\text{-bpmh})_2]$[2] and the dinuclear structure in $[Cd(S_2P(OiPr)_2)_2(4\text{-bpmh})_{0.5}]_2$,[4] 1D coordination polymers with linear chains structure in $[Zn_2(4\text{-bpmh})(2\text{-tpc})_4]_n$, $[Cd(4\text{-bpmh})_2(2\text{-tpc})_2]_n$, $[Cd(4\text{-bpmh})(NCS)_2(DMSO)_2]_n$ and $\{[Zn(4\text{-bpmh})](C_7H_7SO_3)_2(C_2H_5OH)_2\}_n$,[6,7,9] with zigzag chains structure in $[Zn(4\text{-bpmh})(NO_2)_2]_n$,[10] ladder chains structure in $\{[Cd_2(4\text{-bpmh})_3(sac)_4]\cdot 2CH_2Cl_2\}_n$,[14] step-ladder chains structure in $[Cd(S_2P(OiPr)_2)_2(4\text{-bpmh})]_n$,[4] triple and triple-stranded ladder chains structure in $[Zn_6(4\text{-bpmh})_3(p\text{-clba})_6(\mu_3\text{-OH})_4](p\text{-clba})_2\cdot(CH_3OH)$, and $[Zn_6(4\text{-bpmh})_3(p\text{-brba})_6(\mu_3\text{-OH})_4](p\text{-brba})_2\cdot(CH_3OH)$ and $\{[Cd_3(4\text{-bpmh})_3(OAc)_4(NCS)_2(DMSO)_2]\}_n$,[7,8] 2D coordination polymers with layered structure in $\{[Zn(1,3\text{-adaa})(4\text{-bpmh})]\}_n$ and $\{[Cd(1,3\text{-adaa})(4\text{-bpmh})]\}_n$,[20] pillared-bilayer structure in $\{[Zn_2(NH_2\text{-bdc})_2(4\text{-bpmh})]\cdot(H_2O)_4\}_n$ $[Cd_2(isonicotinate)_4(4\text{-bpmh})(H_2O)]_n$,[15,18] double-layered structure in $\{[Zn(1,3\text{-bdc})(4\text{-bpmh})]\cdot 2H_2O\}_n$, $\{[Zn_2(Hnip)(4\text{-bpmh})(nip)_2(\mu_3\text{-OH})]$,[16,22] 2D interpenetration structure in $[Zn_2(sdb)_2(4\text{-bpmh})]\cdot 2DMF$, $[Cd(4\text{-bpmh})(3m\text{-glu})(H_2O)]\cdot H_2O$,[26,28] and 3D coordination polymers with pillared-layer structure in $[Zn_3(cpop)_2(4\text{-bpmh})(H_2O)_2]_n$, $[Cd_3(btc)_2(4\text{-bpmh})_2]$, $\{[Zn(1,4\text{-pdaa})(4\text{-bpmh})]\}_n$, $[Cd_3(4\text{-bpmh})_3(glu)_2(H_2O)_2](NO_3)_2\cdot(4\text{-bpmh})_{0.5}\cdot(H_2O)_8$, $[Zn(pim)(4\text{-bpmh})]$, $[Zn(suc)(4\text{-bpmh})]$, $[Cd_2(oba)_2(4\text{-bpmh})_2]_n\cdot(DMF)_x$, $[Zn_2(oba)_2(4\text{-bpmh})]_n\cdot(DMF)_x$, $[\{Zn(hfipbba)(4\text{-bpmh})_{0.5}\}\cdot H_2O]$, $[Cd(2\text{-}NH_2\text{-bdc})(4\text{-bpmh})_{0.5}]\cdot DMF\cdot H_2O\}_n$,[17,24,28,29,30,33,35] bipillared-layer interpenetrating structure in $[Cd(2\text{-}NH_2\text{-bdc})(4\text{-bpmh})_{0.5}]\cdot DMF\cdot H_2O\}_n$,[35] pillared-bilayer interpenetrating structure in $\{[Cd(bdc)(4\text{-bpmh})]\}_n\cdot 2n(H_2O)$, $\{[Cd(2\text{-}NH_2bdc)(4\text{-bpmh})]\}_n\cdot 2n(H_2O)$, $[\{Cd_2(fdc)_2(4\text{-bpmh})_3\}\cdot 1.5(4\text{-bpmh})\cdot 2(H_2O)]$,[21,23] 3D interpenetrating structure in $[Zn_2(mfda)_2(4\text{-bpmh})]\cdot DMF\cdot H_2O$, $[Cd_2(mfda)_2(4\text{-bpmh})_2]\cdot DMF\cdot H_2O$, $[Zn_2(efda)_2(4\text{-bpmh})]\cdot(DMF)_{0.25}$, $\{[Zn_3(\mu_4\text{-bpdc})_3(4\text{-bpmh})]\cdot 5DMF\}_n$, $\{[Zn_2(\mu_4\text{-bpdc})_2(\mu\text{-bpdb})]\cdot 7DMF\}_n$, and $\{[Zn(4\text{-bpmh})_{0.5}(terep)](H_2O)\}_n$[19,27,34] with assembled 2D bilayers in $\{[Zn(tbip)(4\text{-bpmh})_{1.5}]\ CH_3OH\}_n$.[22] In order to figure out the structure of the mentioned organic ligands and their Zn/Cd coordination structures in combination with 4-bpmh (CCDC reference number), Table S1 has been provided in the Supporting Information.

This results show that the rational choice of organic ligands in combination with 4-bpmh for the design and construction of mixed ligand base coordination compounds with structural and functional diversity is especially challenging. 4-bpmh has been used to generate new coordination compounds with Zn^{2+} and Cd^{2+} containing diverse organic ligands where *β*-diketones are not included. β-diketones has been found to be able to coordinate to the transition metal ions through the chelation of two oxygen atoms of the enolate anion to give tris- and tetrakis(β-diketonato) metal coordination compounds[41–45] The replacement of the C–H bonds with C–F, (fluorinated β-diketonates) makes the β-diketonate unit easier to coordinate with a metal ion and forming an extended conjugated system. For example, an electron-withdrawing perfluoroalkyl group reduces the electron density on the oxygen atoms of β-diketones, and the acidity of the enolic form of these β-diketones is further increased and thereby increasing the Lewis acidity of the metal center in the ensuing metal coordination compound.

Therefore, varying the substituents in β-diketones may cause major changes in the complexes properties like the reactivity against other organic ligands.[46] Typically, the coordination sphere of the metal ion in this case consists of solvent or water molecules, which can be replaced by a variety of mono- or bidentate *N,O,S,P*-donor ligands. Therefore, beside the β-diketones, one neutral bidentate *N,N*-donor linker as a synergic ligand can be a very efficient for manufacturing new multidimensional structures since it completes the inner coordination sphere by binding itself to the metal ions, and keeps the solvent molecules away from the vicinity of the metal ions.[47–49] Therefore, research on the coordination chemistry of β-diketones/4-bpmh is interesting for constructing novel coordination compounds and understanding topology control.

To continue our ongoing research interest in the coordination mode of 4-bpmh and because of the potential applications of these materials in a variety of areas, including optical applications, we have selected two chelating *O,O′*-donor β-diketonates ligands, 4,4,4-trifluoro-1-phenylbutane-1,3-dionate and 1,3-diphenylpropane-1,3-dionate (tfpb, dpp), and one carboxylate, anthracene-9-carboxylate (9-aca) ligand mixed with 4-bpmh to explore new structures of Zn^{2+} and Cd^{2+} transition metal centers of d^{10} electronic configurations (Scheme 1). We succeeded in synthesizing as single crystals the three coordination compounds $[Cd(tfpb)_2(4\text{-bpmh})]_n$ (**1**), $[Cd(9\text{-aca})(NO_3)(OHCH_3)(4\text{-bpmh})]_n$ (**2**), and $[Zn_2(dpp)_4(4\text{-bpmh})]$ (**3**) (Scheme 2)

Result and Discussion

We used here the so called “branched tube technique”, which is simple, cheap, easy-to-use and less reported-on, for the synthesis and growing of single crystals (Figure 1),[50,51] The reaction of $Cd(OAC)_2$ with 4,4-trifluoro-1-phenylbutane-1,3-dionate (tfpb) and $Cd(NO_3)_2$ with Anthracene-9-carboxylate (9-aca) along with 1,2-bis(pyridin-4-ylmethylene)hydrazine (4-bpmh) as a secondary ligand at 60 °C in dry methanol for over a week yielded yellowish block (**1**) and reddish polyhedron (**2**) crystals in the cold arm of the T-tube respectively. To extend the research, we used a similar ligand 1,3-diphenyl propane-1,3-dionate (dpp) and 4-bpmh with $Zn(OAC)_2$ to grow crystals as thin, yellow plates (**3**) in the cold arm of the T-tube. The formula of two 1D coordination polymers $[Cd(tfpb)_2(4\text{-bpmh})]_n$ (**1**), $[Cd(9\text{-aca})(NO_3)(OHCH_3)(4\text{-bpmh})]_n$ (**2**) and the dinuclear coordination complex $[Zn_2(dpp)_4(4\text{-bpmh})]$ (**3**) were derived by X-ray crystallography. Generally, coordination numbers of Cd^{2+} and Zn^{2+} in coordination compounds are four, five, and six.[52] In this work

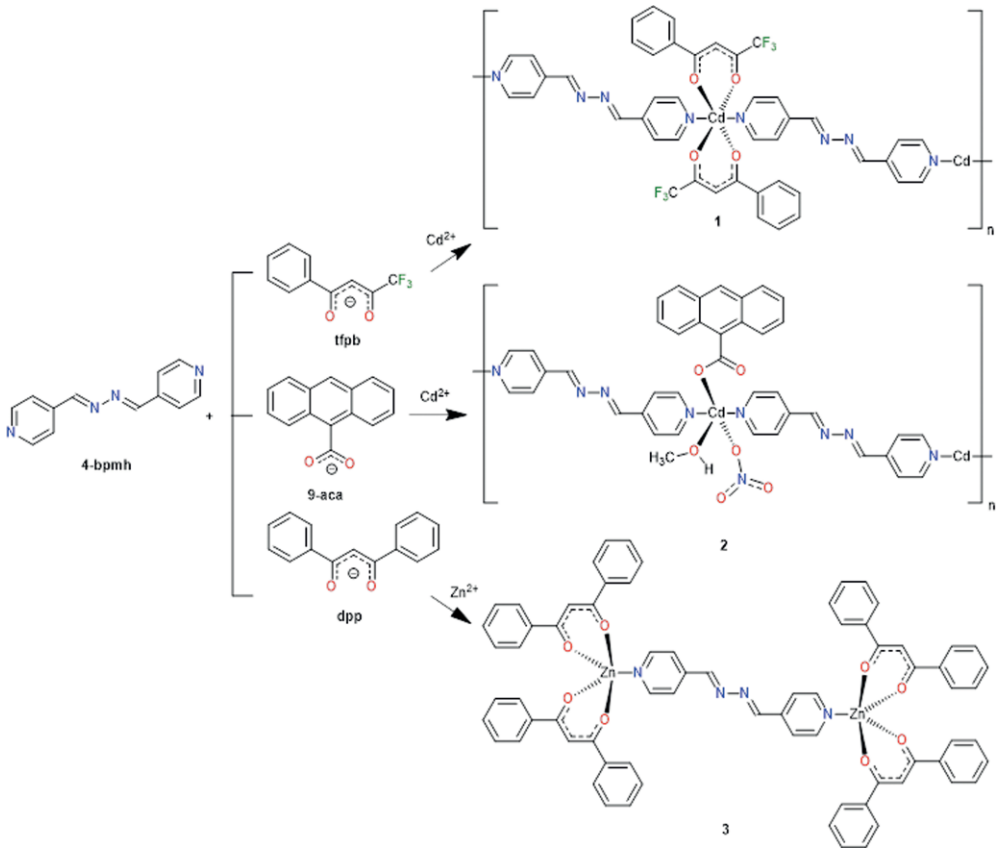

Scheme 2. Synthetic of the coordination compounds **1**, **2**, and **3**.

Cd^{2+} and Zn^{2+} ions have five and six coordinated geometries with octahedral, trigonal bipyramid and square pyramid.

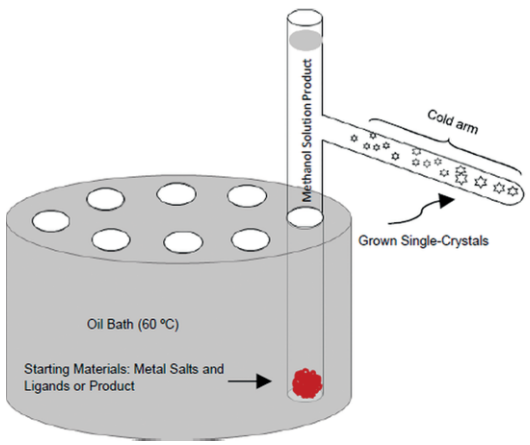

Figure 1. Depiction of the T-tube glass for synthesizing, growing and harvesting of single crystals of metal coordination compounds **1**, **2**, and **3**.

Structure of $[Cd(tfpb)_2(4\text{-}bpmh)]_n$ (1)

Compound **1** crystallizes in the triclinic $P\bar{1}$ space group (see Table S2 for details, Supporting Information). The asymmetric unit contains one half-occupied Cd^{2+} ion on an inversion center, one tfpb and half a 4-bpmh ligand (with an inversion center at the middle of the N–N hydrazine bond). As illustrated in Figure 2, the Cd^{2+} center is ligated by four O atoms from two inversion-symmetry-related chelating tfpb ligands and two N donor atoms from two trans 4-bpmh linkers in a near octahedral coordination geometry. The Cd–N1 bond length is 2.368(9) Å, while the Cd–O1 and Cd–O2 bond lengths are essentially identical with 2.252(7) and 2.256(7) Å. The O(1)–Cd(1)–O(2), O(1)–Cd(1)–N(1), O(2)–Cd(1)–N(1) angles are 82.73(10)°, 88.90(11)° and 94.41(11)° respectively, with deviation from 90°. The distortation from octahedral is due to the different donor atoms and Cd-donor bond lengths and to the constraints on the O–Cd–O angles imposed by the chelation. The close C–C bond lengths of 1.419(6) and 1.378(6) Å in the diketonate ligand show a delocalization of the π electrons over the diketonate group. The bridging nature of the 4-bpmh ligand gives 1D chains and the Cd···Cd distance separated by 4-bpmh is 16.024 Å.

The chains assemble in parallel fashion which neighboring chains being shifted by half of 4-bpmh with respect to each other. There is an interchain hydrogen bonding interaction between an oxygen atom from the diketonate group as acceptor and C-H group from pyridine ring as donor and also short interchain π···π interactions,[53–55] between the diketonate phenyl rings, and interchain C–F···π interactions (Figure 3). Figure 4 shows the crystal packing of **1** along the crystallographic *a* axis. The detailed analysis of short interactions is described in Tables S5, S6, and S8 (Supporting Information).

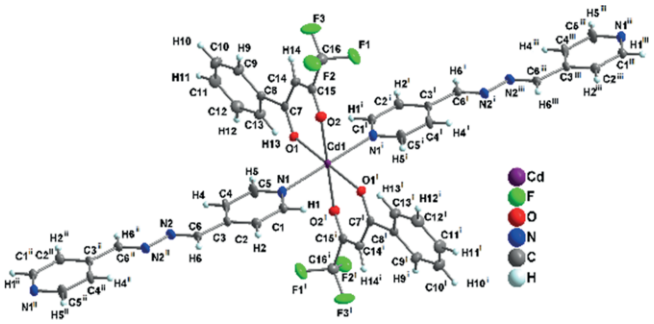

Figure 2. Cd^{2+} ion in **1** with the full set of coordinating ligands. The full labelling Scheme is displayed; the atoms defining the asymmetric unit of the crystal structure are indicated by unprimed labels; displacement ellipsoids at the 50% probability level. Symmetry codes: i = #1 1 –*x*, 1–y, 1 –*z*, ii = #2 –x, 1–y, –z and iii = 1+x, y, 1+z.

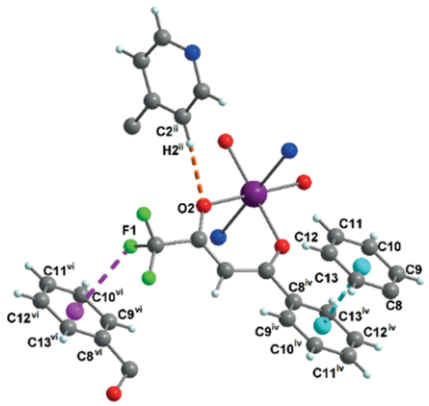

Figure 3. Interchain short interactions including hydrogen bonding (orange), π···π interactions (blue) and C-F···π interactions (pink) among the 1D chain. Symmetry codes #ii -x, –*y* + 1, -z, #iv = 1 –*x*, 2 –*y*, -z, #vi 1 –*x*, 2 –*y*, 1 –*z*.

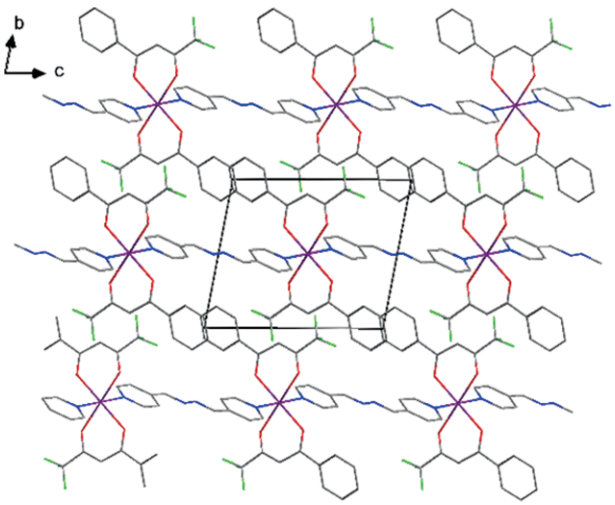

Figure 4. Packing diagram looking against the crystallographic *a* axis of **1**, hydrogen atoms are omitted for clarity. Color legend: Cd (magenta), O (red), N (blue), C (gray).

Structure of [Cd(9-aca)(NO$_3$)(OHCH$_3$)(4-bpmh)]$_n$ (2)

Single crystal X-ray diffraction analysis reveals that **2** crystallize in monoclinic $P2_1/c$ space group (see Table S2 for details, Supporting Information). The asymmetric unit of **2** comprises of one kind of Cd^{2+} ion, one 9-aca that displays as a monodentate ligand, one 4-bpmh bridging linker, one methanol solvent molecule and a monodentate nitrate ion. As illustrated in Figure 5, the Cd^{2+} center is five-coordinate adopting distorted trigonal bipyramid coordination geometry (TBP). Cd^{2+} center is ligated by three different O atoms in the equatorial position belong to the deprotonated carboxyl group of 9-aca, neutral methanol and anion nitrate (O2, O1, and O4) and two N atoms from two trans-positioned 4-bpmh ligands at axial positions with N2–Cd1–N5 angle of 165.30 (4)° (Figure 5).

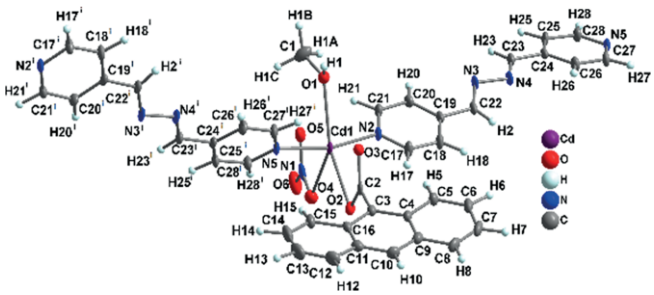

Figure 5. Cd^{2+}ion in **2** with full set of ligands. The full labelling Scheme is displayed; the atoms defining the asymmetric unit of the crystal structure are indicated by unprimed labels; displacement ellipsoids at the 50% probability level; symmetry codes: i = #1 –1+x, 1/2–y, 1/2 + *z*.

The presence monodentate 9-aca and nitrato groups were established by IR and X-ray single crystal analysis in **2**. The pick positions of asymmetric and symmetric stretching vibration band of ν(C=O) group is shifting to the lower frequencies after the formation of the polymer,[56,57] and ν_{asym} and ν_{sym} frequencies appeared at 1581, 1367 cm^{-1} ($\Delta\nu_{asym}$–ν_{sym} = 214), corresponding to the carbonyl functionality of the 9-aca ligand and suggesting a monodentate mode with the Cd–O bond length 2.446(2) Å. The C–O distance for the single bond is 1.423(3) Å, while the C–O distance for the C–O double bond length is 1.283(3) Å. The IR vibrations of nitrate ion with a monodentate binding feature appeared at 1290 cm^{-1} for ν_{sym} (NO_2) with very strong intensity, 1060 cm^{-1} for ν_{sym} (NO_2), 1000 cm^{-1} for ν(NO), and then 739 cm^{-1} for $\delta_{sym}(NO_2)$ with very strong intensity.[58,13]

Selected bond lengths and bond angles for the crystal structure of **2** are given in Table S3 (Supporting Information). The Cd1–N2 and Cd1–N5 bond lengths is 2.1297(17) and 2.0904(18) Å respectively while the Cd1–O1, Cd1–O2 and Cd1–O4 bond lengths are 2.3519(18), 2.4457(17) and 2.601(2) Å. It was found that bond length of Cd–O is notably long (~2.6 Å) indicating a reduced bond valence.[59] According to the VSEPR theory of molecular geometry, an axial position is more crowded because an axial atom has three neighboring equatorial atoms at a 90° bond angle, whereas an equatorial atom has only two neighboring axial atoms at a 90° bond angle and also an equatorial position has two neighboring equatorial atoms at a 120° bond angle.[27] The bulky and sterically hindered 9-aca tended to occupy an equatorial position in monodentate coordination mode along with a methanol and a monodentate nitrate ion therefore, the plane of trigonal con-

sist of three oxygen atoms. The axial positions were occupied by two 4-bpmh which connect metal centers. Therefore, the least electronegative ligands occupy the axial position. But, according to the VSEPR theory of molecular geometry, the axial positions tendency to be occupied by linkers which has a greater electronegativity and pi-electron withdrawing. Hence, a combination of increase in electronegativity and steric hindrance/steric reduction may be responsible for the structural representation found by **2**.

A simplified view of **2** shows, the structure consists of neutral infinite chains of cadmium atoms linked by 4-bpmh bridge that the Cd···Cd distance is 14.794 Å. The overall 1D chain can be easily considered to have sine-wave shape and the complex molecular fragment is [Cd(μ-4-bpmh)(9-aca)(OHMe)(NO_3)]. Figure 6 shows the crystal packing of **2** along the crystallographic *c* axis. In addition, the dihedral angle of two pyridine rings of 4-bpmh is 13.456° (6). Selected torsion angles for the crystal structure of **2**, are given in Table S4 (Supporting Information). The study of the crystal packing of **2** revealed the chains pass through each other like a wave and the stacking of the chains leads to the formation of a channel-like structure filled by anthracene ring along the *a* crystallography axis. There is a stronger hydrogen bonding interaction between nitrate group as acceptor and O–H group from methanol as donor and also two weaker hydrogen bonding interactions in which pyridine ring donate hydrogen-bonds through carbon hydrogen have been detected (Figure 7). We can not find any other effective short interactions. The detailed analysis of short interactions was described in Table S5 (Supporting Information).

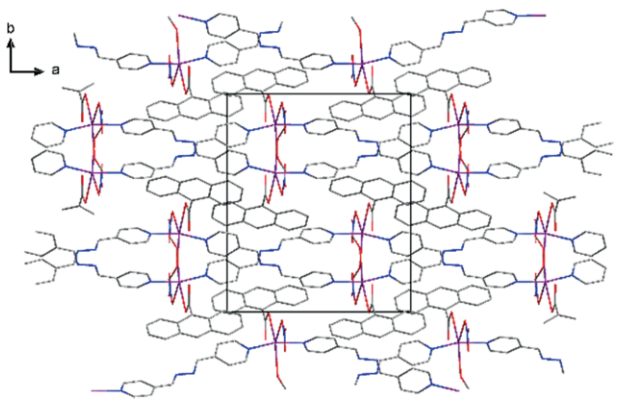

Figure 6. Packing diagram looking along the crystallographic *c* axis of **2**, hydrogen atoms are omitted for clarity. Color legend: Cd (magenta), O (red), N (blue), C (gray).

Structure of [Zn_2(dpp)$_4$(4-bpmh)] (3)

Single crystal X-ray diffraction analysis reveals that **3** crystallize in monoclinic $P2_1/n$ space group (see Table S2 for details, Supporting Information). In fact, the reaction of $Zn(OAC)_2$ with and dpp and 4-bpmh in methanol solution provided a chemically symmetric butterfly-like binuclear coordination structure with molecular formula [Zn_2(dpp)$_4$(4-bpmh)] (**3**). Figure 8 shows asymmetric unit of structure **3**, there is one independent molecule contains two Zn^{2+} ions with same

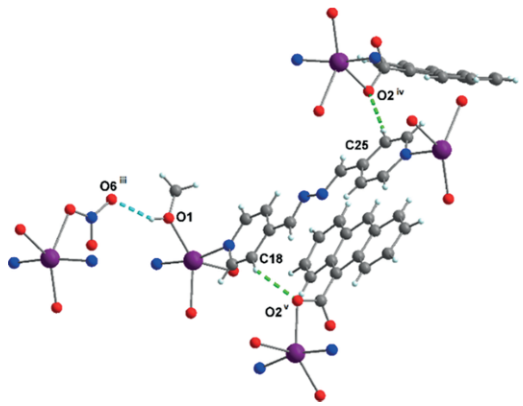

Figure 7. hydrogen bonding interactions between the 1D chains in **2** indicated by green and blue segmented sticks. Symmetry codes #iii = x, –y + 1/2, z + 1/2, iv = –x + 2, y + 1/2, -z–1/2 v = –x + 2, –y, –z.

coordination environment, four dpp ligands, and one μ_2-4-bpmh group bonded Zn^{2+} ions to form [Zn_2(dpp)$_4$(4-BPMH)]. There is one type of metal coordination geometry described as distorted square pyramidal with geometry index τ_5 0.06 and 0.41 (Addison parameter) for both $Zn1^{2+}$ and $Zn2^{2+}$ ions respectively (Figure 9).[60] Each Zn^{2+} center is connected to two dpp forming an inward bent square plane so that 4-bpmh in axial position connect two Zn^{2+} centers. The Zn···Zn distance separated by 4-bpmh is 15.4508(12) Å and the Zn···Zn distance provides an estimate of the length of 4-bpmh.[61]

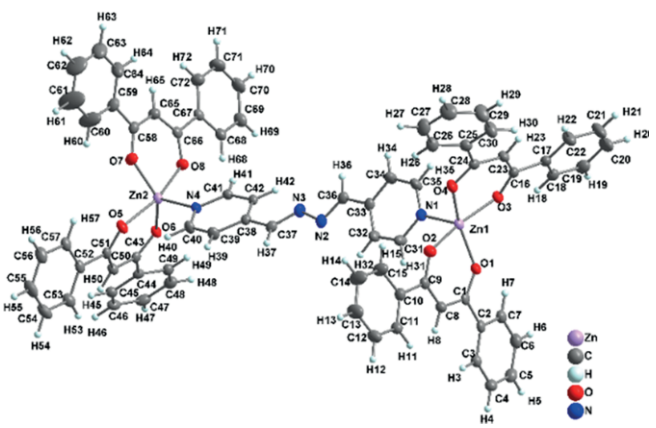

Figure 8. A view of the asymmetric unit of **3** with full Cd coordination along with the labelling Scheme, showing displacement ellipsoids at the 50 % probability level.

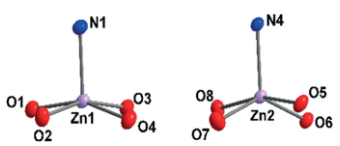

Figure 9. Coordination environment of Zn1 and Zn2 in **3** (50 % probability ellipsoids).

The dihedral angle of two pyridine rings [(N1, C31, C32, C33, C34, C35) and (N4, C40, C39, C38, C42, C41)] of 4-bpmh is 42.456 (120)°. The zinc atoms sit 0.341 and 0.477 Å out of the best plane defined by O1–O2–O3-O4 and O5–O6–

O7-O8 atoms, respectively and the main reason for distortion from the regular square plane is in fact due to intermolecular C-H···O hydrogen bonding and short interactions between aromatic rings (Cg–Cg) and C–H··π interactions of dpp and 4-bpmh of different molecules (Tables S5, S6, and S7 and Figure S1, Supporting Information). The C1–C8, C8–C9, C16–C23, C23–C24, C43–C50, C50–C51, C58–C65 and C65–C66 bond length are 1.406(3), 1.406(3), 1.406(3), 1.395(3), 1.397(3), 1.405(3), 1.398(3), and 1.399(3) Å, respectively, that shows a delocalization of π-electron over diketon groups. Selected bond lengths and bond angles for the crystal structure of **3** are given in Table S3 (Supporting Information). **3** was self-assembled by short interactions described in Tables S5, S6 and S7 (Supporting Information) to form an infinite 3D supramolecular structure in T-form skeleton (Figure S1, Supporting Information). Figure 10 shows crystal packing of molecules along the crystallographic *c* axis and Figure 11 showing intermolecular non-covalent interactions including hydrogen bonding, π···π and C–H···π interactions among molecules.

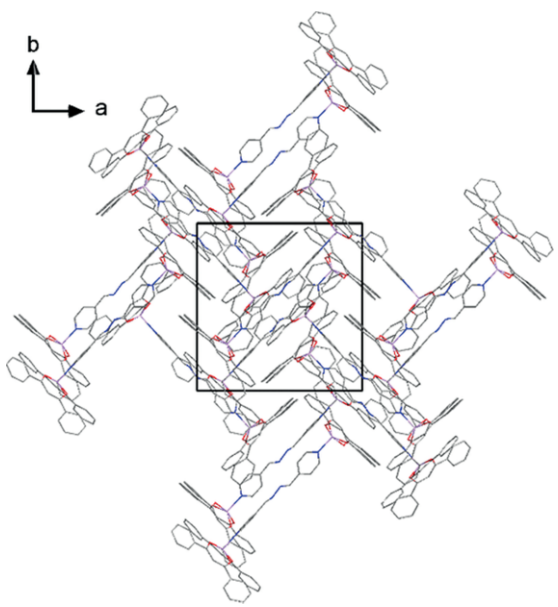

Figure 10. Packing diagram of **3** looking along the crystallographic *c* axis; note the T-form skeleton. Hydrogen atoms are omitted for clarity. Color legend: Zn (pink), O (red), N (blue), C (gray).

Conclusions

Using cadmium(II) nitrate, cadmium(II) acetate, and zinc(II) acetate in appropriate combination with one of the three *O*,*O*′-donor (tfpb, dpp and 9-aca) ligands and one linear neutral bridging *N*,*N*′-donor ligand (4-bpmh, secondary ligand), the new coordination compounds $[Cd(tfpb)_2(4\text{-bpmh})]_n$ (**1**), $[Cd(9\text{-aca})(NO_3)(OHCH_3)(4\text{-bpmh})]_n$ (**2**), and $[Zn_2(dpp)_4(4\text{-bpmh})]$ (**3**) were successfully synthesized under the same experimental conditions. Their single crystals have been grown via branched tube technique and then analyzed by X-ray crystallography. Due to the different shapes, sizes, and coordination abilities of the ligands and metal ions, the metal coordination compounds have different structures. Of *N*,*N*′-donor ligand (4-bpmh) has been investigated in this study, two 1D polymers (**1** and **2**) and a dimeric complex (**3**) formed. 4-bpmh appeared as a bridge ligand in all three structures and *O*,*O*′-donor ligands probably affect the formation of the final structures. The distances between the pyridyl-nitrogen atoms in the 4-bpmh molecule of 11.358 Å for **1** and 10.658 Å for **2** result in a linear and sine-wave 1D chain polymeric topologies respectively. The introduction of fluorine-containing substituents into the β-diketone fragment resulted in the structural changes of a dinuclear coordination complex in **3** to one-dimensional coordination polymer in **2**. This is probably linked to the higher acidity of the enolic form of fluorinated β-diketonate ligands compared to phenyl-substituted β-diketonate which causes the electronic demands of the coordinate. These different structures indicated that the coordination behaviors of metal ions and the coordination modes, different steric hindrances of aromatics played important roles in the construction of final coordination compounds. This study indicates that it is possible to explore interesting aesthetic multi-dimensional structures with chelating β-diketonates along with different neutral *N*,*N*′-donor ligands.

Experimental Section

Synthesis: The title coordination compounds **1**, **2**, and **3** were synthesized from a mixture of one of the metal salts $Cd(OAc)_2$ (0.1 mmol), $Cd(NO_3)_2$ or $Zn(OAc)_2$ (0.1 mmol) with 4,4,4-trifluoro-1-phenylbutane-1,3-dionate (tfpb) (0.2 mmol), anthracene-9-carboxilate (9-aca) (0.2 mmol) or 1,3-diphenylpropane-1,3-dionate (dpp) (0.2 mmol) and 1,2-bis(pyridin-4-ylmethylene)hydrazine as an auxiliary ligand (4-

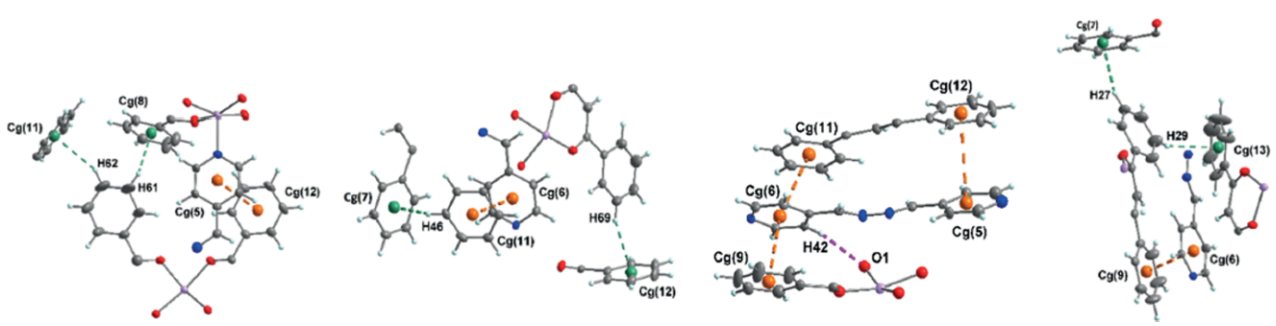

Figure 11. Intermolecular non-covalent interactions including hydrogen bonding (pink), π···π interactions (orange) and C–H···π interactions (green) between molecules. Cg (7) = C2, C3, C4, C5, C6, C7, Cg (8) = C10, C11, C12, C13, C14, C15, Cg (11) = C44, C45, C46, C47, C48, C49, Cg (12) = C52, C53, C54, C55, C56, C57, Cg (13) = C59, C60, C61, C62, C63, C64, Cg (5) = N1, C31, C32, C33, C34, C35, Cg (6) = N4, C40, C39, C38, C42, C41, Cg (9) = C17, C18, C19, C20, C21, C22.

bpmh) (0.05 mmol) (Scheme 2) in a metal-to-ligand ratio of 1:2:0.5 in methanol using a T-tube glass. Figure 1 shows a perspective drawing of the T-tube glass applied. Dried methanol was carefully added to the mixture of starting materials until the arm of the T-tube was completely filled. The tube was sealed and left in an oil bath at 65 °C under silent environment, while the arm was kept at room temperature. Yellow, red and yellow single crystals from **1**, **2**, and **3**, respectively, grew in the cold arm of the tube over a period of one week. Suitable crystals were carefully selected, covered with protective oil and mounted on cryo loops for X-ray analysis. More information about the experimental procedures, instruments used, characterization data and structural characterization of **1**–**3** are provided in the Supporting Information.

Structure Analysis and Refinement: Single crystal X-ray diffraction experiments were performed with protective-oil coated crystals in a cooling gas stream of dry nitrogen [140(2) K] on a Bruker Kappa APEX II CCD diffractometer (Bruker AXS Inc., Madison, WI, USA)[62] with Mo-K_α radiation (microfocus tube, multi-layer mirror system, λ = 0.71073 Å) applying ω-scans. SMART.[63] SAINT[63] and SADABS[64] were used for the calculations of data collection/unit cell refinement, frame integration/data reduction and multi-scan absorption correction, respectively. Maximum and minimum transmission factors are listed in Table S2 (Supporting Information) along with crystal data and further details of data collections and structure refinements.

In the case of **1** the symmetry of the diffraction pattern was compatible with the anorthic space group types $P1$ and $P\bar{1}$. The latter was favored with respect to the value of $|E^2-1|$ and proved to be the correct one in the course of structure refinement, finally. In case of **2** and **3** space group $P2_1/c$ and $P2_1/n$, respectively, was uniquely determined from symmetry and systematic extinctions. Primary structure solutions was achieved by direct methods with SHELXS-97,[65] completion of the structural models including the positions of the hydrogen atom of the hydroxyl group of the coordinating methanol molecule in **2** and most of the other hydrogen atoms in **1**–**3** by subsequent difference-Fourier syntheses calculated with SHELXL-2017.[66] Structure solution with direct methods was not straightforward in the case of **1** and **2**, and subgroup $P1$ and $P\bar{1}$, respectively, was used for solution, followed by transformation to the higher symmetry true space group.[67] Refinement was done by full-matrix least-squares calculations on F^2 using SHELXL-2017[66–68] In the case of **2** the positions of the H atom of the OH group of the methanol ligand and the H atoms at the imino group carbon atoms C22 and C23 were refined. For all other H atoms in **1**, **2**, and **3** the riding model was applied using the program's default idealized C–H bond lengths and N–C–H, C–C–H and H–C–H bond angles where applicable. In addition, the H atoms of the methanol ligand's CH_3 group in **2** were allowed to rotate collectively around the adjacent C–O bond axis. The U_{iso}(H) values were set to $1.5U_{eq}(O_{hydroxyl})$, $1.5U_{eq}(C_{methyl})$ and $1.2U_{eq}(C_{any\ CH\ group})$.

Stabilization of the structural model using appropriate geometrical and anisotropic displacement parameter restraints was needed in the case of **2**, only. In the bridging ligand the pyridyl group containing N5 was subjected to same distance restraints for all C–C bonds. Same distance restraints were also used for C–C bonds of the anthracenyl group of the carboxylate ligand and individual bond lengths restraints were applied for C2–C3, C4–C9 and C11–C16 in this ligand. Finally, all atoms of the anthracenyl group were constrained to be coplanar within the default standard uncertainty, and default "rigid bond" and same U^{ij} components restraints were applied to the atoms of these group. The crystal structure of **3** was shown to contain solvent accessible voids with a volume of 110 Å^3. However, attempts to introduce water molecules to account for some unspecific residual electron density in this region did not result in converging refinement and significant improvement of reliability factors and contribution to $|F_{calc}|^2$ was supposed to be negligible.

In the case of **1** after final refinement the difference electron density map showed residual electron density maxima > 1 e–Å^{-3} in physically not reasonable positions along with several values of $|F_{obs}|^2 >> |F_{calc}|^2$ indicative for unaccounted twinning. Further inspection of the intensity data gave evidence that the crystal under investigation had been suffering from non-merohedral twinning[69] with the twin axis defined as the one parallel to the b^* axis of the anorthic reciprocal unit cell. The twin law (as a rotation matrix written by rows: –1 0 0 –0.789 1 –0.311 0 0 –1) was calculated using the TwinRotMat routine implemented in PLATON and a HKLF5 format data file was created,[67] that allowed for a second, improved refinement assuming the additivity of reflection intensities of the twin components.[70] The twin fraction was refined to 0.76(2)/0.24(2). Graphics of **1**, **2**, and **3** were prepared with DIAMOND.[71]

Crystallographic data (excluding structure factors) for the structures in this paper have been deposited with the Cambridge Crystallographic Data Centre, CCDC, 12 Union Road, Cambridge CB21EZ, UK. Copies of the data can be obtained free of charge on quoting the depository numbers CCDC-1994296 (**1**), CCDC-1991336 (**2**), and CCDC-1991214 (**3**) (Fax: +44-1223-336-033; E-Mail: deposit@ccdc.cam.ac.uk, http://www.ccdc.cam.ac.uk)

Supporting Information (see footnote on the first page of this article): Crystal data and data collection and refinement details of **1**, **2**, and **3** (Table S2), selected bond lengths, angles and torsion angles of **1**, **2**, and **3** (Tables S3 and S4), analysis of hydrogen bonding and ring-interactions (Table S5, S6 and S7), and short intermolecular contacts between molecules of **3** (Figure S1, Supporting Information). Open access funding enabled and organized by Projekt DEAL.

Keywords: Mixed-ligand metal coordination compound; Chelating O,O′-donor β-diketone ligand; O,O′-donor carboxylate ligand; Bridging N,N′-donor ligand; T-tube glass

References

[1] D. M. Ciurtin, Y.-B. Dong, M. D. Smith, T. Barclay, H.-C. zur Loye, *Inorg. Chem.* **2001**, *40*, 2825–2834.
[2] G. A. Brokera, E. R. T. Tiekink, *Acta Crystallogr., Sect. E* **2011**, *67*, m320–m321.
[3] R. Shoshnik, H. Elengoz, I. Goldberg, *Acta Crystallogr., Sect. C* **2005**, *61*, m187-m189.
[4] C. S. Lai, E. R. T. Tiekink, *Z. Kristallogr.* **2006**, *221*, 288–293.
[5] Y. Rachuri, S. Subhagan, B. Parmar, K. K. Bisht, E. Suresh, *Dalton Trans.* **2018**, *47*, 898–908.
[6] V. Lozovan, V. Ch. Kravtsov, E. B. Coropceanu, N. Siminel, O. V. Kulikova, N. V. Costriucova, M. S. Fonari, *Polyhedron* **2020**, *188*, 114702–114714.
[7] B. Notash, M. Farhadi Rodbari, *Polyhedron* **2019**, *171*, 260–268.
[8] S. Islam, J. Datta, F. Ahmed, B. Dutta, S. Naaz, P. Pratim Ray, M. Hedayetullah Mir, *New J. Chem.* **2018**, *42*, 13971–13977.
[9] Q. Wang, B. Liang, J. Y. Zhang, M. Pan, B. S. Kang, C. Y. Su, *Z. Anorg. Allg. Chem.* **2007**, *633*, 2463–2469.
[10] M. Ghoreishi Amiri, G. Mahmoudi, A. Morsali, A. D. Hunterb, M. Zeller, *CrystEngComm* **2007**, *9*, 686–697.
[11] J. Granifo, M. T. Garland, R. Baggio, *Polyhedron* **2006**, *25*, 2277–2283.
[12] S. Halder, A. Dey, A. Bhattacharjee, J. Ortega-Castro, A. Frontera, P. Pratim Ray, P. Roy, *Dalton Trans.* **2017**, *46*, 11239–11249.

[13] G. Zhang, G. Yang, J. S. Ma, *Cryst. Growth Des.* **2006**, *6*, 1899–1902.
[14] S. Kallil, L. Peterson Jr., A. M. Goforth, T. J. Hansen, M. D. Smith, H. C. zur Loye, *J. Chem. Crystallogr.* **2005**, *35*, 405–411.
[15] B. Bhattacharya, R. Haldar, D. K. Maity, T. K. Maji, D. Ghoshal, *CrystEngComm* **2015**, *17*, 3478–3486.
[16] J. Zhou, L. Du, Y. F. Qiao, Y. Hu, B. Li, L. Li, X. Y. Wang, J. Yang, M. J. Xie, Q. H. Zhao, *Cryst. Growth Des.* **2014**, *14*, 1175–1183.
[17] S. Q. Zhang, F. L. Jiang, M. Y. Wu, J. Ma, Y. Bu, M. C. Hong, *Cryst. Growth Des.* **2012**, *12*, 1452–1463.
[18] J. Granifo, Y. Moreno, M. T. Garland, R. Gaviño, R. Baggio, *J. Mol. Struct.* **2010**, *983*, 76–81.
[19] S. Su, C. Qin, Z. Guo, H. Guo, S. Song, R. Deng, F. Cao, S. Wang, G. Li, H. Zhang, *CrystEngComm* **2011**, *13*, 2935–2941.
[20] S. Sanda, S. Parshamoni, A. Adhikary, S. Konar, *Cryst. Growth Des.* **2013**, *13*, 5442–5449.
[21] S. Parshamoni, S. Sanda, H. S. Jena, S. Konar, *Chem. Asian J.* **2015**, *10*, 653–660.
[22] J. Zhou, T. Yan, Y. F. Qiao, Y. D. Zhao, X. Wang, L. Du, M. J. Xie, J. Xu, Q. H. Zhao, *Inorg. Chem. Commun.* **2016**, *73*, 161–165.
[23] D. Singh, C. M. Nagaraja, *Cryst. Growth Des.* **2015**, *15*, 3356–3365.
[24] S. Gholamali Ghomshehzadeh, V. Nobakht, N. Pourreza, P. Mercandelli, L. Carlucci, *Polyhedron* **2020**, *176*, 114265–114271.
[25] N. Rad-Yousefnia, B. Shaabani, M. Zahedi, M. Kubicki, M. Aygün, F. Lloret, M. Julve, A. M. Grzes′kiewicz, M. Sadegh Zakerhamidi, C. Kazakf, *New J. Chem.* **2018**, *42*, 15860–15870.
[26] P. Abdolalian, A. Morsali, G. Makhloufi, C. Janiak, *New J. Chem.* **2018**, *42*, 18152–18158.
[27] B. Fernández, G. Beobide, I. Sánchez, F. Carrasco-Marín, J. M. Seco, A. J. Calahorro, J. Cepeda, A. Rodríguez-Diéguez, *CrystEngComm* **2016**, *18*, 1282–1290.
[28] A. J. Calahorro, E. S. Sebastián, A. Salinas-Castillo, J. M. Seco, C. Mendicute-Fierro, B. Fernández, A. Rodríguez-Diéguez, *CrystEngComm* **2015**, *17*, 3659–3666.
[29] M. Y. Masoomi, A. Morsali, P. C. Junk, *CrystEngComm* **2015**, *17*, 686–692.
[30] S. Singh Dhankhar, M. Kaur, C. M. Nagaraja, *Eur. J. Inorg. Chem.* **2015**, 5669–5676.
[31] M. Y. Masoomi, A. Morsali, P. C. Junk, *RSC Adv.* **2014**, *4*, 47894–47898.
[32] M. Y. Masoomi, S. Beheshti, A. Morsali, *J. Mater. Chem. A* **2014**, *2*, 16863–16866.
[33] M. Y. Masoomi, K. C. Stylianou, A. Morsali, P. Retailleau, D. Maspoch, *Cryst. Growth Des.* **2014**, *14*, 2092–2096.
[34] B. Bhattacharya, R. Haldar, R. Dey, T. K. Maji, D. Ghoshal, *Dalton Trans.* **2014**, *43*, 2272–2282.
[35] R. Haldar, S. K. Reddy, V. M. Suresh, S. Mohapatra, S. Balasubramanian, T. K. Maji, *Chem. Eur. J.* **2014**, *20*, 4347–4356.
[36] S. Parshamoni, S. Sanda, H. S. Jena, K. Tomar, S. Konar, *Cryst. Growth Des.* **2014**, *14*, 2022–2033.
[37] M. Y. Masoomi, S. Beheshti, A. Morsali, *J. Mater. Chem. A* **2014**, *2*, 16863–16866.
[38] Y. Rachuri, B. Parmar, K. K. Bishtc, E. Suresh, *Dalton Trans.* **2017**, *46*, 3623–3630.
[39] Y. Diskin-Posner, G. K. Patra, I. Goldberg, *CrystEngComm* **2002**, *4*, 296–301.
[40] Y. Rachuri, B. Parmar, K. K. Bishtc, E. Suresh, *Dalton Trans.* **2017**, *46*, 3623–3630.
[41] Z. Ahmed, K. Iftikhar, *Dalton Trans.* **2019**, *48*, 4973–4986.
[42] D. N. Bazhin, Y. S. Kudyakova, A. S. Bogomyakov, P. A. Slepukhin, G. A. Kim, Y. V. Burgarta, V. I. Saloutina, *Inorg. Chem. Front.* **2019**, *6*, 40–49.
[43] Y. J. Wang, [d].-F. Wu, J. Gou, Y. Y. Duan, L. Li, H.-H. Chen, H.-L. Gao, J.-Z. Cui, *Dalton Trans.* **2020**, *49*, 2850–2861.
[44] E. A. Varaksina, I. V. Taydakov, S. A. Ambrozevich, A. S. Selyukov, K. A. Lyssenko, L. T. Jesus, R. O. Freire, *J. Lumin.* **2018**, *196*,161–168.
[45] M. Lavanya, M. Jagadeesh, J. Haribabu, R. Karvembu, H. K. Rashmi, P. Uma Maheswari Devi, A. Varada Reddy, *Inorg. Chim. Acta* **2018**, *469*, 76–86.
[46] D. Singh, S. Bhagwan, A. Dalal, K. Nehra, R. K. Saini, K. Singh, S. Kumar, I. Singh, *J. Lumin.* **2020**, *223*, 117255–117263.
[47] V. Lozovan, V. Ch. Kravtsov, E. Gorincioi, A. Rotaru, E. B. Coropceanu, N. Siminel, M. S. Fonari, *Polyhedron* **2020**, *180*, 114411.
[48] S. Muthu, J. H. K. Yip, J. J. Vittal, *J. Chem. Soc., Dalton Trans.* **2001**, 3577–3584.
[49] V. Lozovan, E. B. Coropceanu, P. N. Bourosh, A. Micu, M. S. Fonari, *Russ. J. Coord. Chem.* **2019**, *45*, 13–23.
[50] A. Morsali, M. Yaser Masoomi, *Coord. Chem. Rev.* **2009**, *253*, 1882–1905.
[51] K. Darzinezhad, M. M. Amini, E. Mohajerani, M.-R. Fathollahi, M. Janghouri, B. Notash, A. Rostami, *Z. Anorg. Allg. Chem.* **2020**.
[52] M. Borsari, *Cadmium: Coordination Chemistry*, in *Encycl Inorg Bioinorg Chem.* **2014**, pp.1–16.
[53] X.-J. Yang, F. Drepper, B. Wu, W.-H. Sun, W. Haehnel, C. Janiak, *Dalton Trans.* **2005**, 256–267.
[54] C. Janiak, *J. Chem. Soc., Dalton Trans.* **2000**, 3885–3896.
[55] X. Xu, B. Pooi, H. Hirao, S. H. Hong, *Angew. Chem.* **2014**, *126*, 1307–1311.
[56] K. Nakamoto, *Infrared and Raman Spectra of Inorganic and Coordination Compounds, Part B, Applications*, in *Coordination, Organometallic, and Bioinorganic Chemistry*, 6th edn, Wiley, **2009**.
[57] X. Jia, J. Ma, F. Xia, Y. Xu, J. Gao, J. Xu, *Nat. Commun.* **2018**, *9*, 1–7.
[58] M. Y. Mihaylov, V. R. Zdravkova, E. Z. Ivanova, H. A. Aleksandrov, P. St. Petkov, G. N. Vayssilov, K. I. Hadjiivanov, *J. Catal.* **2020**.
[59] S. Parshamoni, S. Konar, *CrystEngComm* **2016**, *18*, 4395–4404.
[60] A. W. Addison, T. Nageswara Rao, J. Reedijk, J. van Rijn, G. C. Verschoor, *J. Chem. Soc., Dalton Trans.* **1984**, 1349–1356.
[61] W. J. Perkins, T. Maxwell, A. M. Goforth, M. D. Smith, L. Peterson Jr., H. C. zur Loye, *Acta Crystallogr., Sect. E* **2005**, *61*, m2047–m2049.
[62] Bruker AXS, APEX2, Bruker AXS Inc., Madison, Wisconsin, USA, **2012**.
[63] SMART, Data Collection Program for the CCD Area-Detector System; SAINT, Data Reduction and Frame Integration Program for the CCD Area-Detector System. Bruker Analytical X-ray Systems, Madison, Wisconsin, USA, **1997**.
[64] G. M. Sheldrick, in *Program SADABS*: Area-detector absorption correction, University of Göttingen, Germany, **1996**.
[65] G. M. Sheldrick, *Acta Crystallogr., Sect. A: Found. Crystallogr.* **2008**, *64*, 112–122.
[66] G. M. Sheldrick, *Acta Crystallogr., Sect. C: Struct. Chem.* **2015**, *71*, 3–8.
[67] A. L. Spek, *J. Appl. Crystallogr.* **2003**, *36*, 7–13.
[68] C. B. Hübschle, G. M. Sheldrick, B. Dittrich, *J. Appl. Crystallogr.* **2011**, *44*, 1281–1284.
[69] S. Parsons, *Acta Crystallogr., Sect. D* **2003**, *59*, 1995–2003.
[70] P. Müller, R. Herbst-Irmer, A. L. Spek, T. R. Schneider, and M. R. Sawaya, *Crystal Structure Refinement: a Crystallographer's Guide to SHELXL*, IUCr/Oxford University Press **2006**.
[71] K. Brandenburg, DIAMOND (Version 4.0), Crystal and Molecular Structure Visualization, Crystal Impact, Dr. H. Putz & Dr. K. Brandenburg GbR, Bonn Germany, **2009–2018**, http://www.crystalimpact. com/diamond.

Received: September 29, 2020